Journal of Cultural Heritage 22 (2016) 956–967

Available online at
ScienceDirect
www.sciencedirect.com

Elsevier Masson France
EM|consulte
www.em-consulte.com/en

Original article

Indoor microclimatic study for Cultural Heritage protection and preventive conservation in the Palatina Library

Carla Balocco[a], Giuseppe Petrone[a,*], Oriana Maggi[b], Giovanna Pasquariello[c], Roberto Albertini[d], Cesira Pasquarella[e]

[a] Department of Industrial Engineering, University of Florence, Via Santa Marta, 3, 50139 Firenze, Italy
[b] Department of Environmental Biology, "Sapienza" University of Rome, Largo Cristina di Svezia, 24, 00165 Roma, Italy
[c] Central Institute of Graphic Arts, Ministry of Cultural Heritage, Activities and Tourism, Via della Lungara, 23, 00165 Roma, Italy
[d] Department of Clinical and Experimental Medicine, University of Parma, Via Gramsci, 14, 43124 Parma, Italy
[e] Department of Biomedical, Biotechnological and Translational Sciences, University of Parma, Via Volturno, 39, 43125 Parma, Italy

ARTICLE INFO

Article history:
Received 16 December 2015
Accepted 23 May 2016
Available online 16 June 2016

Keywords:
Microclimatic conditions
Conservative preservation
Indoor air quality
Paper conservation
CFD

ABSTRACT

We suggest a method to identify the suitability of a chosen indoor environment for paper material conservation in historical libraries. Our approach is based on two steps: numerical simulation for solving the air velocity, moisture and temperature fields, and then post-processing indexes evaluation to assess how the indoor microclimatic conditions can be favourable or not to the growth and development of microorganisms responsible for paper deterioration. A real case study was analysed in two different conditions: one the present situation and the other proposed by the authors with a HVAC system assuring controlled air temperature and RH levels. Numerical models, validated by experimental data published in previous works, were used to carry out microclimatic results. Starting from these results, some indexes suggested by the scientific literature were computed to check the suitability of the indoor environment for preserving a library heritage. Boolean parameters were also deduced from the combination of microclimatic factors favouring the growth of microorganisms responsible for paper material deterioration. Our research can provide a methodological approach that predictively allows one to know when, where and how the processes responsible for indoor microorganism activity can find the microclimatic conditions for their kick-off and triggering, and then their areas of potential growth. The proposed method highlights the main causes of the deterioration processes connected to building thermo-physics. Simulation results turned out to be a fundamental approach to identify the risky zones and potential areas of triggering deterioration processes of all the materials present.

1. Research aims

Our present research was based on a multidisciplinary approach including biological and microclimatic analysis associated with the application of the Computational Fluid Dynamic (CFD). The aim of our research was to investigate how indoor microclimatic conditions can facilitate microorganisms' growth and in consequence determine unfavourable conditions for paper material conservation. We developed numerical models for simulating microclimatic conditions in one archive in the historical *Palatina Library*, in Parma (Italy), under two different conditions. The first one referred to the real condition of the historical archive (no HVAC system present); in the second one we assumed the room was equipped by an ideal standard HVAC system, assuring controlled indoor climatic conditions. Transient simulations were carried out, allowing one to compute some derived indexes widely used in the literature for quantifying adequate microclimatic conditions with respect to the most common deterioration processes of library heritage. Boolean indexes were also proposed to identify critical zones and surfaces triggering deterioration processes, as well as the optimal microclimatic conditions over time for heritage protection.

2. Introduction

Microclimatic conditions affect conservation and maintenance of libraries, archives and museums, especially in historical

* Corresponding author. Tel.: +39 3383 063032.
E-mail addresses: carla.balocco@unifi.it (C. Balocco), giuseppe.petrone@unifi.it (G. Petrone), oriana.maggi@uniroma.it (O. Maggi), giovanna.pasquariello@beniculturali.it (G. Pasquariello), roberto.albertini@unipr.it (R. Albertini), ira.pasquarella@unipr.it (C. Pasquarella).

http://dx.doi.org/10.1016/j.culher.2016.05.009
1296-2074/

Fig. 1. De Rossi room – photo.

buildings [1–3]. A great amount of research highlights the effects between cyclic variations of indoor conditions, outdoor climate and environmental pollution, mechanical stresses, chemical and thermo-physical changes of building materials with significant deterioration and biodegradation processes on cultural heritage in libraries, historical exhibitions and museums [4–6]. In particular, a comprehensive study of the interaction between indoor and outdoor climate fluctuations is shown in [5]. Degradation effects due to outdoor/indoor pollution have also been investigated by experimental measures and numerical models solved by CFD tools [7]. New conditioning plant installation suitability in heritage buildings has been widely discussed [8,9]. An impressive study on heat and moisture induced strain to historical wooden materials is shown in [10]: a hygrothermal building dynamic simulation is combined with FEM multiphysics numerical modelling for indoor climatic condition assessment and thermo-physical response of wooden materials. The acclimatization of sensitive heritage objects to the environment within which they were preserved for a long time, has been extensively used to establish climate control criteria [11–14]. This concept has been explicitly expressed in many standards that suggest the optimal ranges of thermo-hygrometric parameter values for preventive cultural heritage conservation [15–21] and in recent studies that posit the concept of "historic climate" [13,14]. Many studies have investigated degradation and deterioration phenomena due to mechanical stress, chemical and photochemical reactions and biological mechanisms [22–26]. Most of them attribute heritage cellulosic material bio-deterioration to air temperature and humidity fluctuations [27–29]. A crucial study on deterioration processes caused by physical and biological agents connected to the indoor microclimatic but also water distribution (as an indirect measure of the well-known "water activity" index, based on non-destructive techniques) is reported in [30].

The importance of a multidisciplinary investigation to guarantee stability requirements of microclimatic conditions for conservation in libraries and archives is shown in [31,32]. Variations in thermo-physical parameters must be reduced, because they are as damaging as their absolute values [8,32]. Recent research has provided useful methods to evaluate the so-called "building-plant system capacity" [33], and passive reactive technique application for climate and Indoor Air Quality (IAQ) monitoring using risk indexes [3,34].

Starting from the above studies and recent research [34], we investigated the indoor microclimatic variations linked to building thermo-physics that can create unfavourable conditions for paper material conservation and facilitate microorganism growth. This study was carried out in the Palatina Library in Parma (Italy). Microclimatic parameters, airflow, moisture transport phenomena and microorganism potential growth were investigated and compared for two conditions: one, the present situation without any plant system, and the other, proposed by the authors with an optimal, standard HVAC system.

3. Modelling

3.1. System configurations

The *De Rossi* archive room (Fig. 1) was the case study. It has a global volume of 496 m^3, 6.90 m wide and 12 m long and a cross-vaulted ceiling. Two walls of the room are internal partitions and the others face the external environment. One of the external walls, South-West oriented (48.28 m^2), has a central window of 3.5 m^2; the wider external wall (42.20 m^2) is South-East oriented. The room has restrictions on reader access, visitor number reduction, and absence of activities, which could influence indoor pollutant concentrations. Physical and microclimatic parameters were collected during monitoring campaigns discussed in [34]. A solid model was built-up considering one person standing inside and a second one sitting. Fig. 2 shows: exterior walls and indoor partitions, air volume shaped at the top under the ceiling vault, main furniture (desk, wooden ladders) and two occupants. The wooden shelving perimeter containing books, a window, a linear shaped aluminium lighting body and lamp were also modelled (Fig. 3). A second version of this geometry was set-up, introducing an HVAC system that is based on a constant air volume (CAV) central beam ceiling solution. This solution was chosen because of its minimum architectural impact with respect to other plant typologies, and its guarantee of potential reversibility and maintenance facility. Fig. 4 shows the outlined ceiling beam, with air ducts, air supply and return diffusers and an integrated lighting system. The proposed ceiling beam provides 4 air changes per hour, introducing 1800 m^3/h of fresh air for a ratio of 3, between fresh and recirculated air. The ratio between the recirculated and total airflow rate (induction rate) is 0.25.

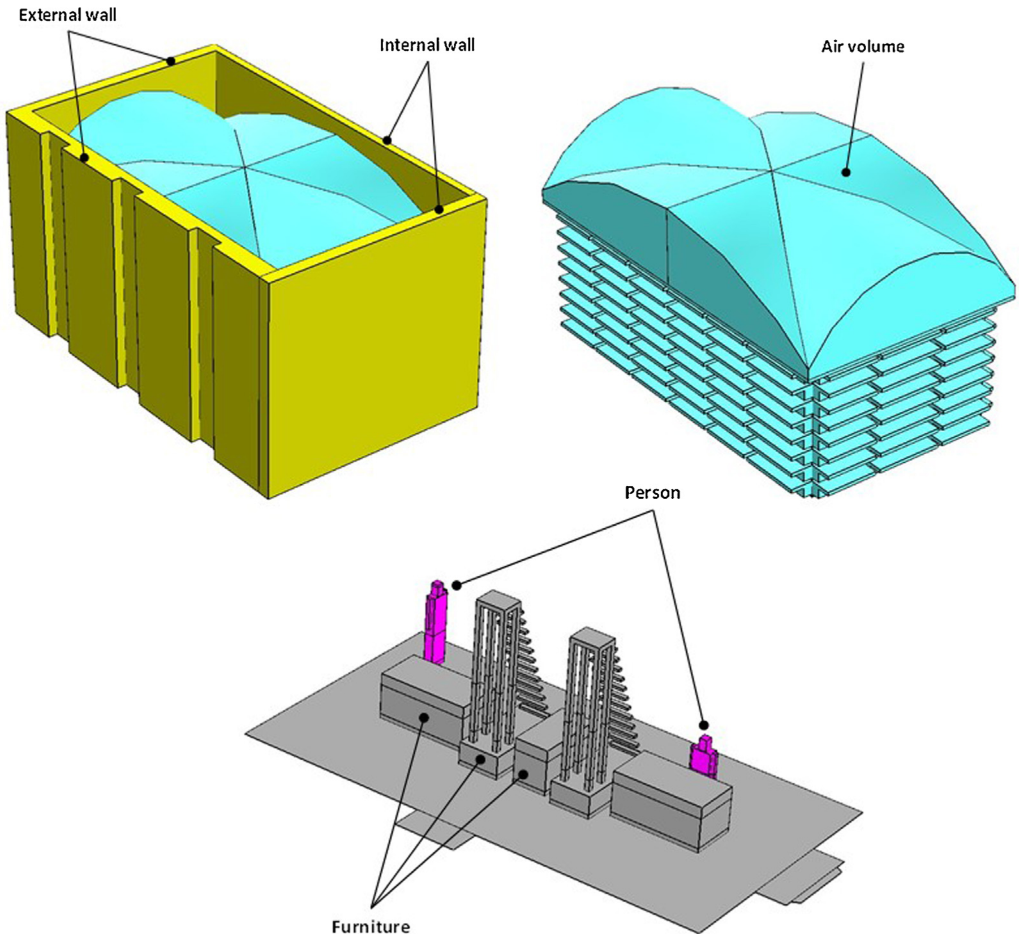

Fig. 2. Numerical model geometry. Walls (yellow), air volume (cyan), main furniture in the centre of the room (gray) and people (magenta).

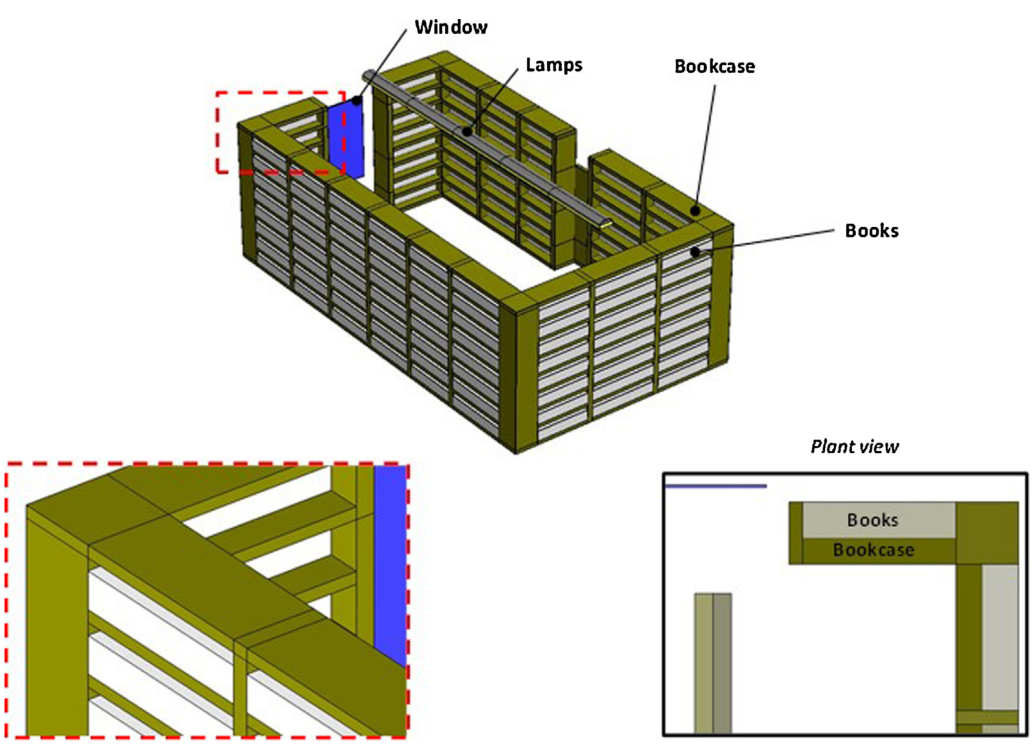

Fig. 3. Numerical model geometry: wooden shelving perimeter (in mustard) containing books (light grey), a window (in blue), a linear shaped aluminium lighting body (dark grey) and lamp (yellow).

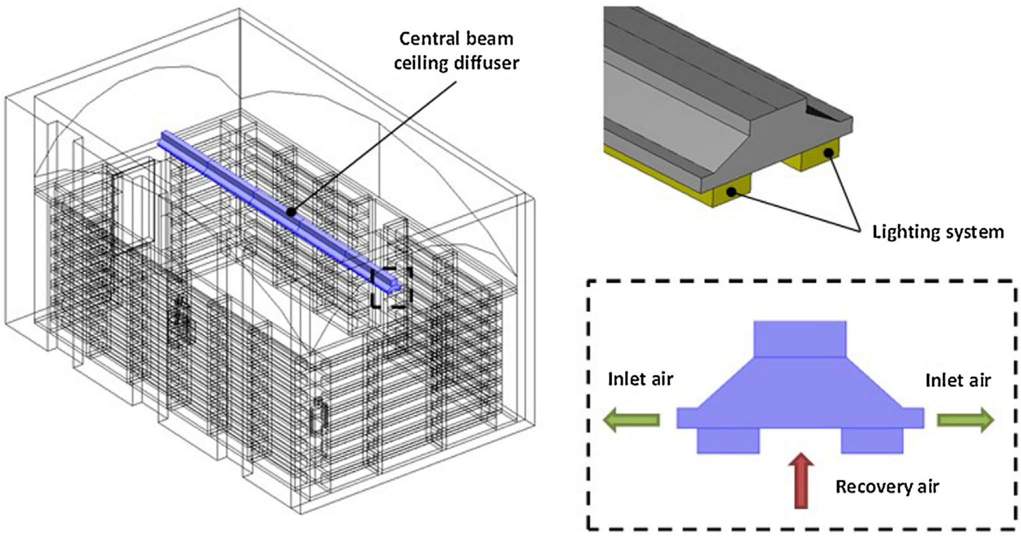

Fig. 4. Central ceiling beam air diffuser considered in the numerical model to simulate the proposed HVAC system.

3.2. Governing equations

The airflow inside the room was solved by numerical integration of the Reynolds Averaged Navier-Stokes equations under the assumption of Newtonian fluid and uncompressible flow. Momentum equations were coupled with a standard k-ε model [35,36] applied as a closure scheme for turbulence modelling. Additional passive-scalar equations were used to solve the thermo-hygrometric variable. The temperature was evaluated by solving the energy equation. Moisture transfer phenomena were approached choosing relative humidity (RH) as a dependent variable and adopting an Euler-Euler scheme to simulate its transport and diffusion in the air [37]. The generic formulation of the partial differential equation considered is:

$$\frac{\partial(\rho\phi)}{\partial t}+\nabla\cdot(\rho\phi U)=\nabla\cdot(\Gamma\nabla\phi)+\Delta \quad (1)$$

with ρ fluid density, U velocity vector, Γ diffusion coefficient and Λ source term. Table 1 shows, for each specific governing equation, the symbols used in Eq. (1). The first analysed configuration is based on a natural convection driven flow, while the second refers to a forced ventilating system. For this last case, the air inlet velocity is 0.83 m/s, with inlet temperature of 18 °C in winter and 24 °C in summer. RH at inlet section was set at 50% for both seasons. These inlet conditions were chosen to obtain set-point values according to the present target standard as the best compromise for paper collection and wooden material [15–21]. For both configurations, external climatic conditions used correspond to the “typical days” whose climatic hourly data were processed according to [38] for Parma (Italy). From all the climatic data, the average annual air temperature is 14.5 °C, the maximum of all the hourly temperature values is 37.7 °C and minimum is −5 °C. Therefore, a typical day for the worst summer conditions, the one with maximum air temperature value (22 July), and the typical day for the worst winter conditions, the one with minimum temperature value (20 January), were selected. The computed trends expressing time-evolution of solar-air temperature and RH were used as boundary conditions applied to the external walls. The solar-air temperature is the temperature that the external air must have to exchange the same thermal convective flux, with the wall surface, that is on the other hand exchanged by convection and solar radiation [39–41]. Five linear module lamps (50 W each), people (daily occupancy schedule: 10–12 hours and 16–18 hours) and thermo-hygrometric conditions of the adjacent conditioned rooms to the one studied, were considered. For these rooms, transient conditions linked to the present fan-coil regulation system were implemented with a control of two (winter) and three (summer) different levels of set-point temperature (T_int), and a constant 50% RH. Applied levels for (T_int) were: for the winter configuration 18 °C (8–18 hours) and 15 °C (19–7 hours); for the summer configuration 22 °C (8–18 hours), 26 °C (19–2 hours) and 24 °C (3–7 hours). Sensible heat and vapour flux released by occupants are linked to the above cited schedules (58 W metabolic sensible heat and 4.2E-2 g/(m^2·s) vapour flux for each person standing). Physical properties of materials are listed in Table 2.

3.3. Numerical solution

Continuous equations with boundary conditions were spatially discretized by using a Finite Elements (FE) approach on non-structured grids of second order tetrahedral elements. Steady state solutions of discrete equations were carried out by applying an iterative dumped Newton-Raphson scheme [36,42] based on discretized PDE linearization by a first-order Taylor expansion. Algebraic equation systems were solved with the PARDISO package, used to solve unsymmetrical sparse matrixes by an LU decomposition method. The convergence criterion was set to 1E-5. Time integration of governing equations, for transient simulations, was performed with an implicit differential-algebraic solver [42], solving at each time step, the nonlinear equation system. Transient simulations were carried out using [43] and a workstation of two 64-bit 6-core/12-thread processors, 2.3 GHz of frequency and 128 GB of RAM. All the calculations were initialized using, as initial distribution of dependent variables, the solution of the same model at stationary conditions and corresponding to the their value assumed at the initial time of transient simulations, to get a periodic stabilized regime over a not too long time period. Using a suitable “guest” to initialize each transient analysis (that means a distribution of air velocity, temperature and relative humidity at time = 0), corresponding to a steady state solution of the system obtained for assigned values of each time-dependent boundary condition (i.e. the external temperature) set to its initial value, allows one to remove any “inertial” effect of the system. For this purpose, this procedure is very often used in this kind of transient numerical analysis. All the simulations were carried out for a period of

Table 1
Terms used in Eq. (1) depending on specific variable.

Equation	ϕ	Γ	Λ
Continuity	1	0	0
Momentum	$\mathbf{U}$	$\mu+\mu_T$	$-\nabla p+\mathbf{F}_g$
Turbulent kinetic energy	k	$\mu+\frac{\mu_T}{\sigma_k}$	$\frac{1}{2}\mu_T\left[\nabla U+(\nabla U)^T\right]^2-\rho\varepsilon$
Dissipation rate of kinetic energy	ε	$\mu+\frac{\mu_T}{\sigma_\varepsilon}$	$\frac{1}{2}C_{\varepsilon 1}\frac{\varepsilon}{k}\mu_T\left[\nabla \boldsymbol{U}+(\nabla \boldsymbol{U})^T\right]^2-\rho C_{\varepsilon 2}\frac{\varepsilon^2}{k}$
Energy	T	$\frac{\lambda}{C_p}$	$\frac{Q}{C_p}$
Relative humidity	RH	$\rho\left(-\delta_p p_{sat}/\xi-D_w\right)$	0

Table 2
Physical properties of materials used in the numerical models.

Material	ρ [kg/m^3]	η [Pa s]	k [W/(m K)]	C_p J/(kg K)	ξ [kg/m^3]	δ_p [kg/(m s Pa)]	D_w [m^2/s]
Wall	1600	–	0.47	840	0.0068	3.1E-11	4.23E-6
Glass	2500	–	1.00	800	0	0	0
Wood	500	–	0.50	1000	0.086	4.5E-11	6.14E-7
Paper	940	–	0.12	1340	0.097	2.3E-11	3.16E-6
Person	950	–	0.62	4180	–	–	–
Air	$p/(RT)$	5E-5	0.04	1004	0.028	1.9E-10	2.59E-5

12 days (i.e. adopting the chosen cyclically 24-hour variation of each time-dependent boundary condition) for each considered season (winter/summer) and system configuration (with or without an HVAC system).

3.4. Model validation

To assure mesh-independent results, a grid test was preliminarily made by evaluating the simulation result variation (e.g. air velocity magnitude, temperature and RH) in a chosen spatial position of the model, increasing the number of elements of the computational grid. Table 3 provides absolute deviation and normalized variance of the values compared to those obtained with the finest mesh (*MESH#3*). It can be realized that, over a certain value of mesh refinement, relative variance is lower than 10% for velocity magnitude, i.e. the most sensitive variable with respect to mesh size. Simulation models were also validated by comparing numerical results with the in depth experimental data analysis and processing presented in [34]. Fig. 5 shows an extract of the validation procedure, where time-evolution of experimental detected temperature and RH, at a chosen spatial location, are reported against results obtained by the numerical model: a good agreement was found.

4. Post-processing indexes

Post-processing of dependent variables (U, magnitude of air velocity vector; T, temperature; RH, relative humidity) allowed the evaluation of some derived parameters indicating suitability conditions for microorganism (fungi and bacteria) growth and proliferation. Knowing air temperature, velocity and humidity distribution, some further results were obtained by using some indexes suggested in the literature to correlate the thermo-hygrometric indoor conditions.

The first parameter we considered is the "water activity number", a_w, defined as the ratio between the partial vapour pressure of water in a substance and the standard state partial vapour pressure of water [44–46], as follows:

$$a_w = p/p_{sat} \tag{2}$$

where p and p_{sat} are respectively the value of pressure and the saturation pressure at the same temperature. In food science engineering, the standard state is most often defined as the partial vapour pressure of pure water at the same temperature, then pure distilled water has a_w equal to one [44], and the a_w is used because it provides useful information on the conditions for a possible presence of nutrients for microorganisms. The a_w value is always between 0 (substance without water content) and 1 (water). In the ambient air, at a chosen equilibrium state (that means psychrometric conditions far enough from saturation) water activity corresponds to the relative humidity (RH).

Referring to transient simulation results, in order to correlate the building thermo-physical behaviour and indoor microclimatic conditions (being outside the limit values suggested by the standards for conservation and preventive protection of the cultural heritage), a "Damage Index" (defined from now on as DI) allowing different fungal species proliferation and development, was also proposed. This index is Boolean, and its value 1 is given by a combination of humidity and temperature conditions compatible with several fungal species potential growth. The humidity conditions are related to high rates of RH, or water activity numbers for materials potentially at risk. The considered a_w range variation was defined as $0.7 < a_w < 1$. Temperature conditions were otherwise related to low values, referring to a temperature range of $-5 < T < 15$ (°C). Analytically, the Boolean value of the proposed index DI assumed value "1" (true) if variable a_w and T are both inside the previously defined range, otherwise it would assume value "0" (false). The values of T and RH intervals corresponding to DI = "true" were chosen since they correspond to significant fungal proliferation index values as already highlighted in [47–49]. The DI = "true" index indicates all those areas, referring to the isopleths proposed by Sedlbauer and reviewed by other authors [50–52], where germination rates can be even less than 2 days for organic materials belonging to the substrate-group I (biologically recyclable building materials) and the increase in surface thickness of mould be equal to 4 mm/day.

In addition, by means of a search in the literature, we found that the influence of temperature on the bacteria growth rate can be correlated by means of the same Arrhenius formula used in chemical kinetics to connect the reaction rate with temperature. Starting from these studies on Arrhenius law applications, another parameter was derived, i.e. the logarithmic growth rate (G). The bacteria logarithmic growth rate G was computed referring to [53–55], as expressed below:

$$G = -\mu/(2.303 \cdot R \cdot T) \tag{3}$$

Eq. (3) is used to describe, for a defined temperature range, the exponential trend of the bacteria growth rate with temperature [53]. G is the logarithmic growth rate, μ is the temperature

Table 3
Influence of spatial discretization on numerical model results.

	DOF (10^6)	DOF increasing (%)	U			T			RH		
			Value [m/s]	Absolute gap [m/s]	Relative gap [–]	Value [°C]	Absolute gap [°C]	Relative gap [–]	Value [–]	Absolute gap [–]	Relative gap [–]
MESH #1	1.903	–	1.2E-02	4.8E-03	28.2%	17.7	6.3E-02	0.36%	50.02%	5.5E-05	0.01%
MESH #2	2.389	25.5	1.6E-02	1.3E-03	7.9%	17.8	2.5E-03	0.01%	50.01%	3.4E-06	0.00%
MESH #3	3.416	43.0	1.7E-02	0.0E+00	0.0%	17.8	0.0E + 00	0.00%	50.01%	0	0.00%

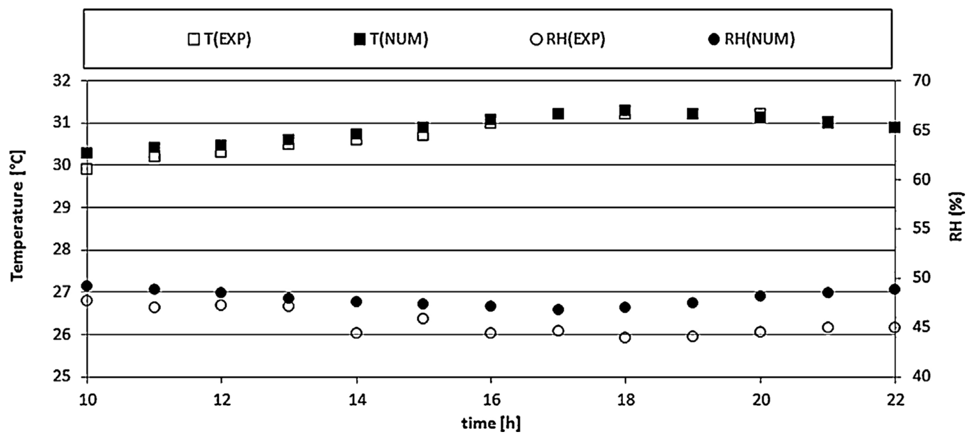

Fig. 5. Experimental (EXP) and numerical (NUM) time-evolution of temperature (T) and relative humidity (RH) at a chosen location of the studied room.

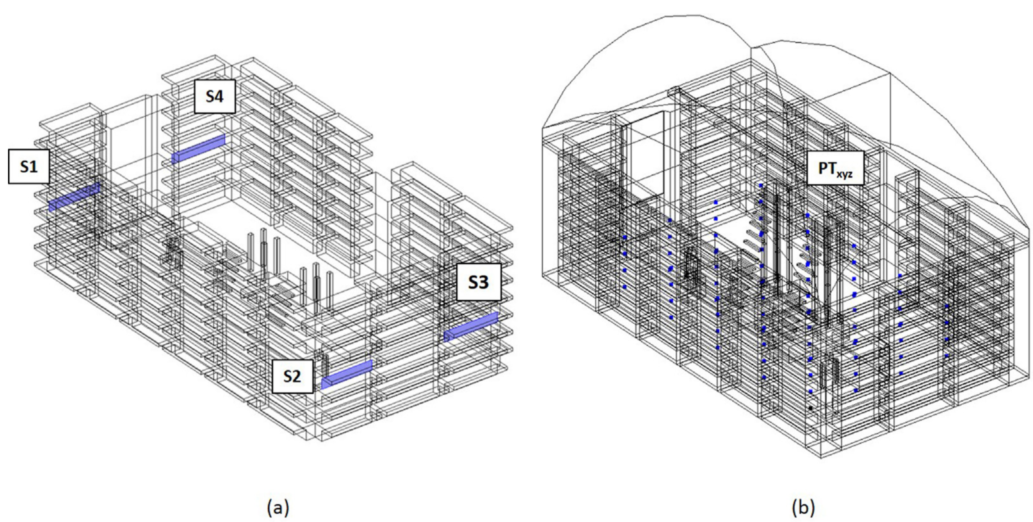

Fig. 6. The 4 surfaces (S1,. . .,S4) location as "reference surfaces" for carrying-out some synthetic results (a); grid of chosen points used for the EDT evaluation (b).

characteristic (that is a constant value for a class of bacteria), R is the ideal gas constant and T the temperature in Kelvin. The number 2.303 is a conversion factor between the Neperian and base 10 logarithms. As a matter of fact, the G formula is expressed by the base 10 logarithm, while the ordinary differential equation ($dN/dt = kN$), that statistically defines the growth rate of any N population is in general expressed by a Neperian logarithm ($G' = \ln(k)$). The logarithmic scale provides a linear correlation between parameter G and the local temperature. According to its suggested original description [54,55], we expressed μ in kcal/mol. Expression of μ in kcal/mol has a "historical" reason apart from of a real "physical" one [53–55]. The logarithmic growth rate was calculated for assigned values of the parameter μ, corresponding to a given class of bacteria species, as provided in [53–55]. The thermal characteristic (μ) values chosen for G calculation were considered for microorganism classes, i.e. the $G_{\mu 10}$ index refers to all kinds of bacteria with a thermal characteristic up to $\mu = 10$, exploiting indications given in [54]. Following this approach, evaluation of G allows identification of objects and surfaces that have an average temperature favourable to the growth of all bacteria species with a thermal assigned μ characteristic. The chosen values of μ were 10, 20, 30 kcal/mol, and the corresponding logarithmic growth rates were listed as $G_{\mu 10}$, $G_{\mu 20}$ and $G_{\mu 30}$. Once the values of G had been computed, applying the NISO TR01-1995 method [18], the "relative degradation rate" at different temperatures was also calculated. The NISO standard suggests evaluation of the "relative degradation rate" (ΔG_{μ}) as the difference between growth rate G calculated on a chosen surface under study and its value calculated for the

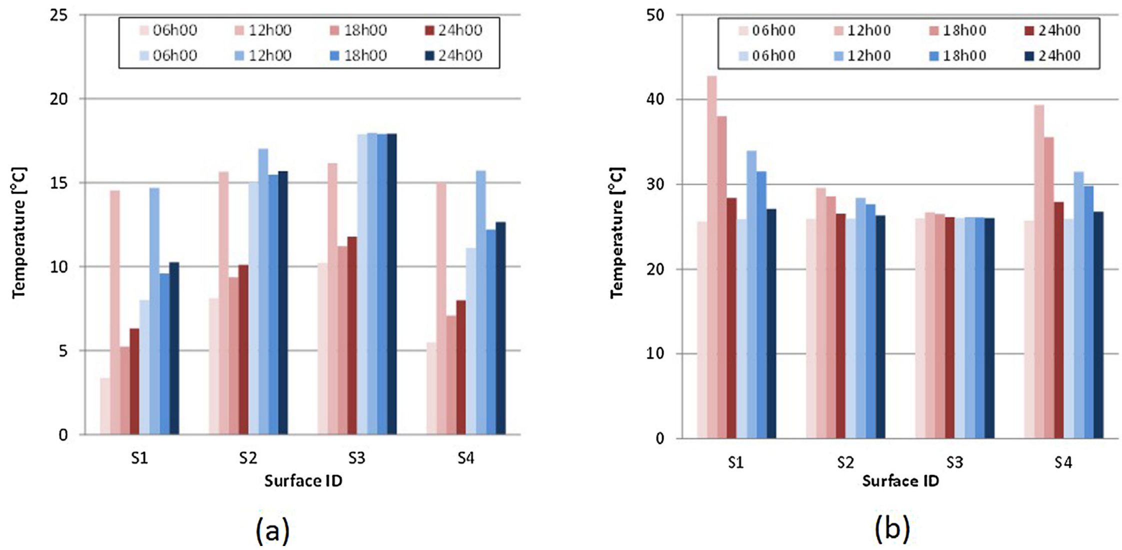

Fig. 7. Average temperature calculated on the S1,. . .,S4 surfaces at different time instants in winter (a) and summer (b) typical day, for the HVAC(N) (red bars) and HVAC(Y) (blue bars) configurations.

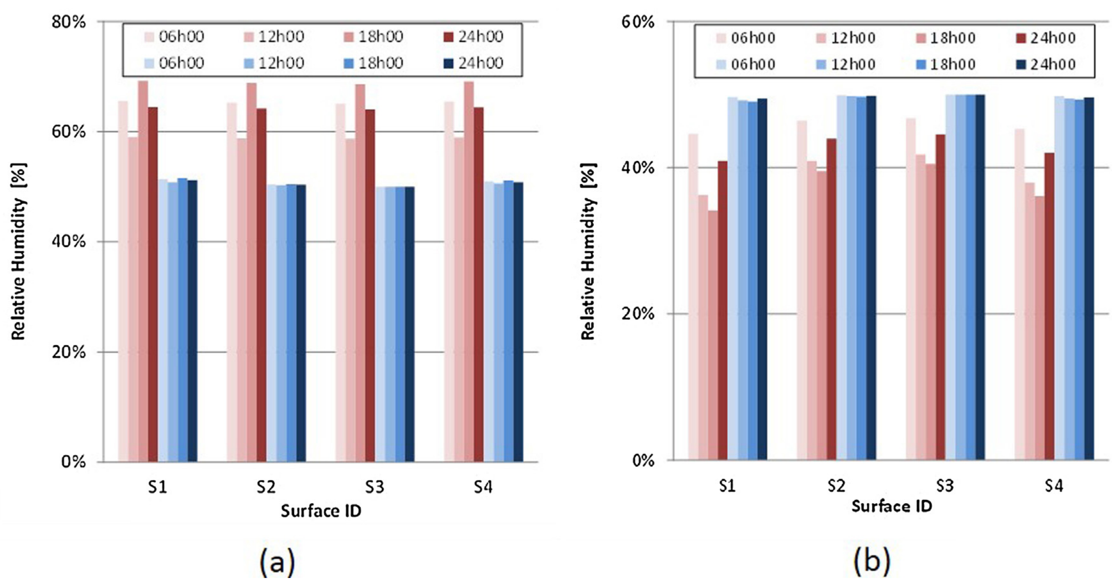

Fig. 8. Average relative humidity evaluated on the S1,. . .,S4 surfaces at different time instants in winter (a) and summer (b) typical day, for the HVAC(N) (red bars) and HVAC(Y) (blue bars) configurations.

reference conditions (corresponding to T = 21 °C and RH = 50%). This procedure was applied in our investigation for each considered value of the thermal characteristic (μ), that means computing the "relative degradation rate" for several classes of bacteria.

To check the correct air distribution, proper ventilation and thermal comfort in the indoor environment, the Air Diffusion Performance Index (ADPI) was calculated according to [56]. This index gives useful information about air distribution in different zones of the same space strictly connected to ventilation effectiveness and condensation and mould phenomena control. A basic definition of ADPI is given in ASHRAE [56], which statistically relates the space conditions of temperature and air velocity for thermal comfort in cooling: high ADPI values are desirable which correspond to high comfort levels due to good ventilation air mixing. The ADPI values were computed referring to a chosen number of discrete points in the room (a grid of 80 points). The grid's nodes correspond to coordinates $x = 2 \div 6.5$ (step 1.5); $y = 2 \div 10$ (step 2); $z = 0.5 \div 2$ (step 0.5). The ADPI index was computed as the percentage of the 80 test points for which the Effective Draft Temperature takes on values included in ($-1.5\,K < EDT < 1.0\,K$). The EDT expression used was the one suggested in [57]:

$$EDT = (T - T_{sat}) - 8 \cdot (U - 0.15) \quad (4)$$

When EDT is between -1.5 K and $+1.0$ K a high percentage of occupants feel comfortable, there are optimal conditions for proper ventilation of the room and the risk of condensation and mould growth, fungal spore transport through building structures but also moisture sorption or desorption and mechanical deformation of materials, are the lowest.

5. Results

All results presented from now on, refer to the 12th day of simulation. Results on the airflow field are due to natural convection effects when the De Rossi Room was considered at the present state, which means without any ventilating and air

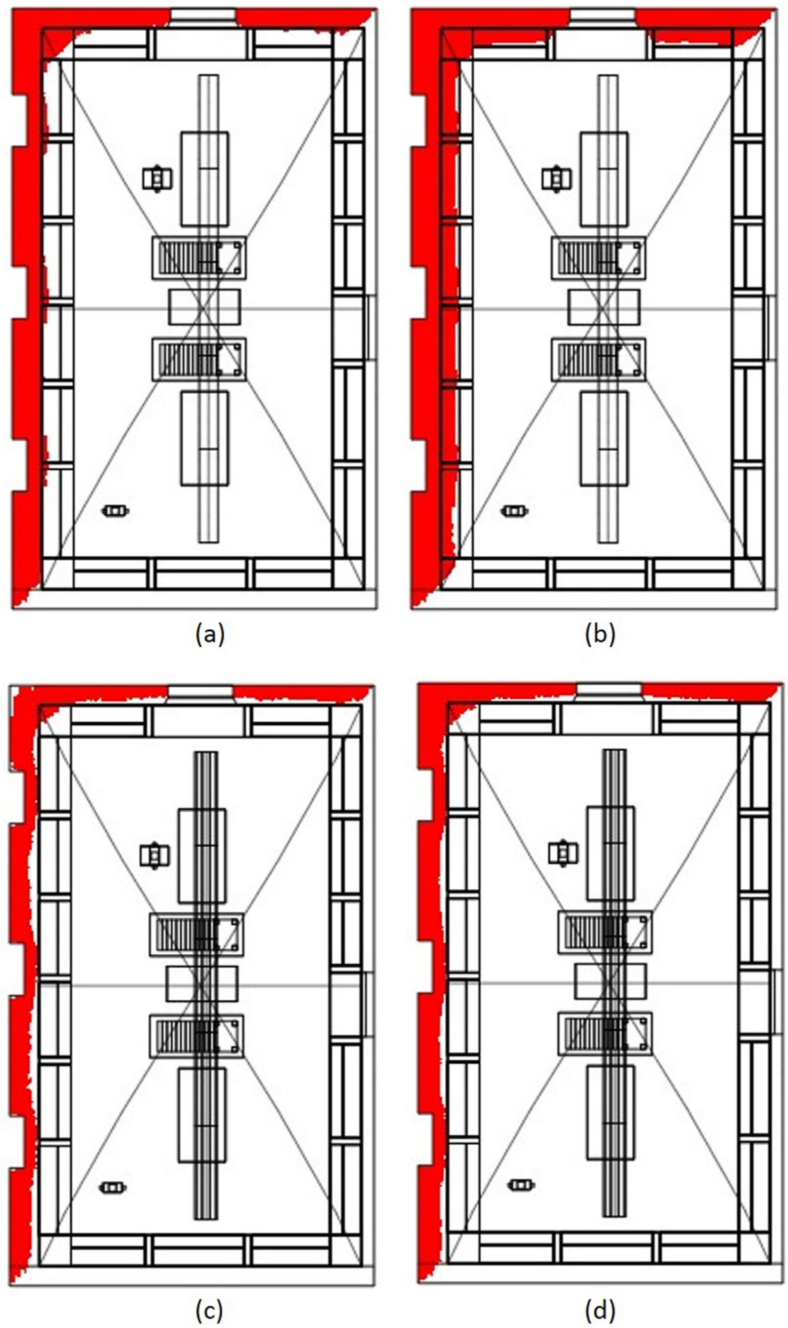

Fig. 9. Value “true” (in red) for the DI computed on a horizontal slice (2 m from floor) for winter typical day at 7 hours in the HVAC(N) (a) and HVAC(Y) (b) configurations, and at 22 hours in the HVAC(N) (c) and HVAC(Y) (d) configurations.

conditioning system (from now on, called HVAC(N)). As described in [58], the airflow was thermally driven by the combined effect of internal heat sources and external constraints. A thermal plume, located in people proximity, determined a weak local air motion directed towards the ceiling. Global flow patterns resulted from a combination between this flow and a second one, due to different thermal conditions between the external and internal walls. Because of summer/winter conditions, the second air flow recirculation, presented opposite rolling directions: the hottest walls were the external ones, so that air moved upward close to them; otherwise they became the coldest ones, so that air tended to move downward in their proximity. Results on velocity, temperature and RH distribution on transverse and longitudinal slices of the room are reported in [31,32]. Analysing the simulation results of the plant solution, the effect of the ceiling beam on airflow, temperature and RH distribution appears very important. When if the room were to be equipped with an HVAC system (from now on HVAC(Y)) the velocity fields would almost totally driven by the inlet and recovery conditions and the buoyancy contribution would no longer be appreciable. The flow patterns reflect this item, being globally shaped in the form of rolling convective rolls with longitudinal axes with respect to the room geometry. Despite the ventilating system, air velocity in proximity of the bookcases appears anyway very low. Streamlines of flow computed in one time instant given in a transverse section and the air velocity distribution magnitude in one horizontal and one vertical slice are provided as supplementary online material to this paper, as well as the spatial distribution of temperature and relative humidity that appear almost homogeneous, highlighting a good mixing effect by the ventilating incoming air.

6. Discussion

A quantitative comparison of values assumed by the above mentioned indexes between the HVAC(N) and the HVAC(Y) configuration of the room is now discussed. As introduced, we investigated two specific microclimatic conditions: the present climate inside the room and that supplied by a plant providing the microclimatic conditions proposed by Italian and International standards for preventive protection and conservation. The two conditions were not analysed as "consequential" to each other, but rather as "opposed". This allows "objective" deduction of the difference between the present microclimatic conditions and those reachable by respecting the standards in a different set-up of the room by means of forecasting simulations. From an operative point of view, we retained four specific surfaces (vertical back surfaces of stored books), defined as "reference surfaces", in order to analyse and compare the results obtained (Fig. 6a) between the different set-ups.

The authors' decision to provide results belonging to the 4 representative surfaces was necessary so as to give a summary of results. The reference surfaces (S1,. . ., S4) were chosen because they represent the variability of the microclimatic conditions of the room correlated with its thermo-physical performance. Actually, the room has two walls facing outwards and two partitions facing internal zones. This is why surfaces close to the four corners of the room were selected. In a similar manner, in order to perform a comparative analysis, we held the same grid of points used for the EDT computation (Fig. 6b) for the different set-ups investigated.

The bar diagrams in Fig. 7 show the average temperature computed on S1,. . ., S4 in 4 different timings. Diagrams are plotted for HVAC(N) and HVAC(Y) configurations in typical winter and summer day conditions. Similarly, Fig. 8 provides the average RH evaluated on the reference surfaces. As can be noticed, the plant solution contributes to breaking down minimum and maximum temperature peaks, in winter and summer conditions, respectively. However, surfaces close to external walls of the room (S1 and S4) are significantly subjected to the sudden environmental climatic variations over time even in the HVAC(Y) configuration, especially in winter. From the RH point of view, the HVAC(Y) assures much more stable conditions throughout the day and in every considered location. It appears that (see Fig. 8) in winter, differences in RH values are of several percentage points between configurations HVAC(N) and HVAC(Y). Differences were found to be slighter in summer when the HVAC system guarantees RH distribution, variation control and stability: it is always maintained at 50% (configuration HVAC (Y)). The composed Fig. 9 (from up-left-up-right to down-left-down-right) shows, in a horizontal section of the room (2 meters from the floor), the zones where DI assumes value "true" (value 1, represented in red). Using horizontal slices to plot the DI relates to the fact that near the perimeter of the room temperature T and relative humidity RH gradients, along the vertical direction are minimal as compared to those on horizontal planes. Our proposed Boolean index provides the opportunity of assessing "at first sight" whether the potentiality of a chosen area is favourable or not to fungi/mould germination. The expression of the damage index DI (Boolean "true" or "false") allowed graphic plotting of the assumed value. DI was plotted referring to a typical winter day, for two most critical hours of the day (7 and 22 hours) with respect to the external constraint (worst combination between T_ext and RH_ext), and for the HVAC(N) and HVAC(Y) configurations. For HVAC(N), i.e. the room's present state, DI value "true" appears not only in the wall stratigraphy, but also in correspondence of computational domains including the shelves and books. This means dangerous and risky conditions (i.e. potential environmental conditions favourable to fungi/mould development and growth) even inside the books. Relative degradation rates were also calculated (Table 4) as previously described. In particular, the adopted procedure for the evaluation of the values in Table 4, is listed below:

- calculation of the average surface temperature for the reference surfaces (S1,. . .,S4) at a specific time instant;
- calculation of growth rate G by Eq. (3) using the values of thermal characteristics (μ) corresponding to each class (10, 20, 30) and the temperature values given in point 1;
- calculation of reference growth rate (G_{ref}), using Eq. (3) using the values of thermal characteristics (μ) corresponding to each class (10, 20, 30) and the temperature value of 21 °C, as given in NISO standard [18];

Table 4
Relative degradation rates ($\Delta G\mu$) computed for different activation energy (μ) at different locations (S1,. . .,S4) for several time instants and for the HVAC(N) and HVAC(Y) configurations.

t	S1 (%)	S2 (%)	S3 (%)	S4 (%)
HVAC(N)				
$\Delta G\mu_{10}$				
6 hours	1.7	1.8	1.8	1.7
12 hours	4.9	2.8	2.0	4.5
18 hours	4.3	2.5	2.0	3.9
24 hours	2.5	2.0	1.9	2.3
$\Delta G\mu_{20}$				
6 hours	3.1	3.3	3.3	3.2
12 hours	9.1	5.1	3.7	8.3
18 hours	7.9	4.6	3.6	7.2
24 hours	4.5	3.6	3.4	4.3
$\Delta G\mu_{30}$				
6 hours	4.2	4.5	4.5	4.3
12 hours	12.6	6.9	5.0	11.5
18 hours	11.0	6.3	4.9	10.0
24 hours	6.2	4.9	4.6	5.9
HVAC(Y)				
$\Delta G\mu_{10}$				
6 hours	1.8	1.8	1.8	1.8
12 hours	3.6	2.5	1.9	3.2
18 hours	3.2	2.3	1.8	2.8
24 hours	2.1	1.9	1.8	2.0
$\Delta G\mu_{20}$				
6 hours	3.2	3.3	3.3	3.3
12 hours	6.7	4.5	3.4	5.8
18 hours	5.8	4.2	3.4	5.2
24 hours	3.9	3.5	3.3	3.7
$\Delta G\mu_{30}$				
6 hours	4.4	4.5	4.5	4.5
12 hours	9.3	6.2	4.6	8.0
18 hours	8.0	5.7	4.6	7.1
24 hours	5.3	4.8	4.5	5.1

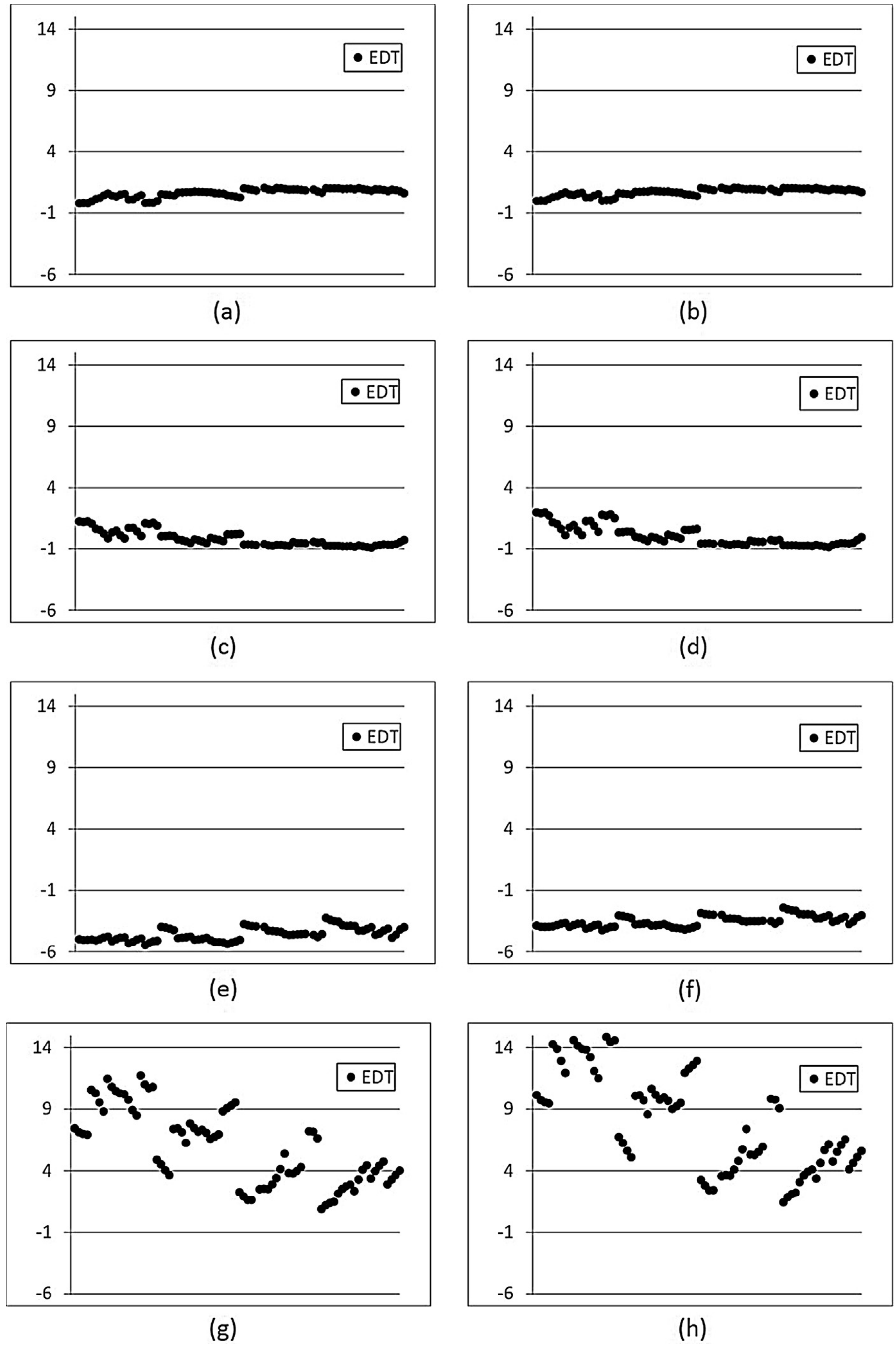

Fig. 10. EDT values for: (a) HVAC (Y) – winter – 11 hours (ADPI 85%), (b) HVAC (Y) – winter – 15 hours (ADPI 80%), (c) HVAC (Y) – summer – 11 hours (ADPI 89%), (d) HVAC (Y) – summer – 15 hours (ADPI 83%), (e) HVAC (N) – winter – 11 hours (ADPI 0%), (f) HVAC (N) – winter – 15 hours (ADPI 0%), (g) HVAC (N) – summer – 11 hours (ADPI 1%), (h) HVAC (N) – summer – 15 hours (ADPI 0%).

- calculation of "relative degradation rate" (G-G_{ref}) as a percentage difference between value of G referring to the single surface (point 2 in the list) and the reference one (point 3 in the list).

The above procedure was repeated for both climatic conditions (summer/winter) and for both conditions of the room (HVAC(N), HVAC(Y)), with the purpose of monitoring the differences. Therefore, starting out from the evaluation of the surface temperature in one area (e.g. S1, a predictive simulation in this case, but, when available, an experimental acquisition), at a particular time instant (e.g. 22.00 hours), for the connected external microclimatic conditions (e.g. winter), and in the use conditions of the room (e.g. HVAC(N)), the procedure allows evaluation of whether the specific area taken as a sample is a potential risk area for bacteria growth. Table 4 gives values of G at the specified locations S1,. . .,S4 and for different time instants. Results appear in compliance with values suggested by the Standards: values obtained with the HVAC(Y) are always the lowest, except in rare cases for 6:00 a.m., for which however they are close to those obtained in the HVAC(N) configuration.

Some composed graphs (Fig. 10, from up-left-up-right to down-left-down-right) quantify EDT values and their dispersion with respect to comfort conditions (i.e. range $-1.5 < EDT < 1$). The EDT values, for the two different conditions, were calculated using air temperature and velocity values corresponding to 80 points distributed (as nodes of a 3D grid) in the room. Therefore, 20 points were considered, for instance, for each assigned value of the coordinate *x* (4 values) along the *y* direction for *z* included between 0 and 2 metres. The 80 point grid, taken as a sample for calculation of the EDT index, "occupies" practically all the volume of the room accessible to people. Results were computed for time corresponding to human presence (11 and 15 hours), in winter and summer and, of course, for HVAC(N) and HVAC(Y). EDT results considering the HVAC(Y) condition were very good: the percentage of points within the range $-1.5 < EDT < -1$ was from 80 to 89%, which means ADPI values from 80 to 89%. HVAC(N) results (corresponding values at the considered points) were still out of range (ADPI from 0% to 1%) and at least in winter were still around the value minus 5, but during summer they are fully dispersed, presenting higher values also around 15. This fact must be understood as the highest discomfort index and also the particular condition of strong indoor thermo-hygrometric variations potentially dangerous for all the items. This is not a guarantee for conservation, also because of potential "mechanical" stress induced on the same constituent elements and components (i.e. wood and paper).

7. Conclusions

In this study, a model corresponding to the present microclimatic conditions of the Palatina Library was implemented (HVAC(N)). Results were compared with experimental data allowing a numeric model validation based on measured data. This model was then used for forecasting type analyses concerning a different set-up of the room (HVAC(Y)). The main aim of the study consisted of a comparison of the two simulated microclimatic conditions and specifically of the indexes of potential start up and growth of microorganisms (especially fungi and bacteria) responsible for the deterioration of the heritage items in the room. Our study highlights how any conditioning plant installation in heritage buildings can be accurately evaluated in comparison with microclimatic conditions provided by the present situations of the building. In particular, the suggested indexes, "quantitatively" compared, contribute to the identification of the potentially favourable and unfavourable microclimatic conditions for the growth and development of fungi and bacteria, the cause of deterioration of the heritage items preserved in the room. The two conditions (the present state without a plant and the proposed ideal standard state with a plant) were analysed not as "consequential" but rather as "opposed" situations. For this purpose, transient simulations were initialized by stationary solutions of the velocity fields, air temperature and relative humidity carried out by using assigned values of the external climatic parameters (identical for both configurations) corresponding to the thermal-fluid-hygrometric constraint condition at the initial instant of the transient analysis considered. This procedure allowed "objective" deduction of the difference between the present microclimatic conditions and those reachable by respecting the standards. Finally, the proposed method based on CFD transient simulations and post-processing index evaluation, can be used for any similar cases for which it is crucial to evaluate the environmental climate quality and the suitability of a plant system to control and assure over time, stable conditions in contrast to the outdoor climatic parameter impulsive variations. For this purpose, the method allows one to assess plant-building system integration to guarantee thermo-hygrometric quality of the library and archive environments, but also to define forecasting assessment for preservation and protection of the cultural heritage from deterioration processes and microorganism growth.

Appendix A. Supplementary data

Supplementary data associated with this article can be found, in the online version, at http://dx.doi.org/10.1016/j.culher.2016.05.009.

References

[1] D. Camuffo, Microclimate for cultural heritage, Elsevier, Amsterdam, 1998.
[2] D. Camuffo, Indoor dynamic climatology: investigation on the interaction between walls and indoor environment, Atmos. Environ. 17 (1983) 1803–1809.
[3] M. La Gennusa, G. Rizzo, G. Scaccianoce, F. Nicoletti, Control of the indoor environments in historical buildings: experimental measurements in an old Italian museum and proposal of a methodology, J. Cult. Herit. 6 (2005) 147–155.
[4] F. Karaca, An AHP-based indoor air pollution risk index method for cultural heritage collections, J. Cult. Herit. 16 (2015) 352–360.
[5] M. Andretta, F. Coppola, L. Seccia, Investigation of the interaction between the outdoor environment and the indoor microclimate of a historical library, J. Cult. Herit. (2015), http://dx.doi.org/10.1016/j.culher.2015.07.002.
[6] M. Strada, A. Carbonari, F. Peron, L. Porciani, P. Romagnoni, The microclimate analysis of tezone "105" of the Venetian Arsenale, J. Cult. Herit. 3 (2002) 89–92.
[7] S. Albero, C. Giavarini, M.L. Santarelli, A. Vodret, CFD modelling for the conservation of the Gilded Vault Hall in the Domus Aurea, J. Cult. Herit. 5 (2004) 197–203.
[8] D. Camuffo, A. Bernardi, G. Sturaro, A. Valentino, The microclimate inside the Pollaiolo and Botticelli rooms in the Uffizi Gallery, Florence, J. Cult. Herit. 3 (2002) 155–161.
[9] F. Romano, L.P.M. Colombo, M. Gaudenzi, C.M. Joppolo, L.P. Romano, Passive control of microclimate in museum display cases: a lumped parameter model and experimental tests, J. Cult. Herit. 16 (2015) 413–418.
[10] Z. Huijbregts, H. Schellen, J. van Schijndel, B. Ankersmit, Modelling of heat and moisture induced strain to assess the impact of present and historical indoor climate conditions on mechanical degradation of wooden cabinet, J. Cult. Herit. 16 (2015) 419–427.
[11] S. Michalski, The ideal climate, risk management, the ASHRAE chapter, proofed fluctuations, and towards a full risk analysis model, in: Proceedings of Experts' Roundtable on Sustainable Climate Management Strategies. Alternative Climate Controls for Historic Buildings, Tenerife, ed. F. Boersma, Getty Conservation Institute, Los Angeles, 2009.
[12] S. Nava, F. Becherini, A. Bernardi, A. Bonazza, M. Chiari, I. García-Orellana, F. Lucarelli, N. Ludwig, A. Migliori, C. Sabbioni, R. Udisti, G. Valli, R. Vecchi, An integrated approach to assess air pollution threats to cultural heritage in a semi-confined environment: the case study of Michelozzo's Courtyard in Florence (Italy), Sci. Total Environ. 408 (2010) 1403–1413.
[13] F. Becherini, A. Bernardi, M.C. Di Tuccio, A. Vivarelli, L. Pockelè, S. De Grandi, S. Fortuna, A. Quendolo, Microclimatic monitoring for the investigation of the different state of conservation of the stucco statues of the Longobard Temple in Cividale del Friuli (Udine, Italy), J. Cult. Herit. 18 (2016) 375–379.
[14] A. Bernardi, D. Camuffo, M. Del Monte, C. Sabbioni, Microclimate and weathering of a historical building: the ducal palace in Urbino, Sci. Total Environ. 46 (1985) 243–260.
[15] MIBAC, D.M. 10 maggio 2001. Atto di indirizzo sui criteri tecnico-scientifici e sugli standard di funzionamento e sviluppo dei musei (Art. 150, comma 6, del D. Leg. n. 112 del 1998). G.U. 19 Ottobre 2001, n. 244, S.O. Italian Standard.
[16] ASHRAE Standard 62, Ventilation for Acceptable Indoor Air Quality, ASHRAE Standards, USA, 2001.
[17] ASHRAE, Museums, libraries and archives, in ASHRAE Handbook: Heating, Ventilating, and Air-Conditioning Applications, SI edition, Atlanta, 2003.
[18] NISO TR0, Environmental Guidelines for the Storage of Paper Records, A technical Report by W.K. Wilson, NISO, Maryland, USA, 1995.
[19] UNI 10829, Beni di interesse storico e artistico – Condizioni ambientali di conservazione – Misurazione ed analisi, Italian Standard, 1999.
[20] UNI EN 15757, Conservation of Cultural Property Specifications for temperature and relative humidity to limit climate-induced mechanical damage in organic hygroscopic materials. English version, 2010.
[21] UNI 10969, Beni Culturali. Condizioni ambientali di conservazione. Principi generali per la scelta ed il controllo dei parametri microclimatici in ambienti interni, Italian Standard, 2002.
[22] H. Brandl, A. von Däniken, C. Hitz, W. Krebs, Short-term dynamic patterns of bioaerosol generation and displacement in an indoor environment, Aerobiologia 24 (2008) 203–209.
[23] B. Lighthart, B.T. Shaffer, Viable bacterial aerosol particle size distributions in the midsummer atmosphere at an isolated location in the high desert chaparral, Aerobiologia 11 (1995) 19–25.
[24] K.H. Bartlett, S.M. Kennedy, M. Brauer, C. van Netten, B. Dill, Evaluation and determinants of airborne bacterial concentrations in school classrooms, J. Occup. Environ. Hyg. 1 (2004) 639–647.
[25] A.L. Pasanen, P. Pasanen, M.J. Jantunen, P. Kalliokoski, Significance of air humidity and air velocity for fungal spore release into the air, Atmos. Environ. 25 (1991) 459–462.
[26] C.F. Green, P.V. Scarpino, S.G. Gibbs, Assessment and modeling of indoor fungal and bacterial bioaerosol concentrations, Aerobiologia 19 (2003) 159–169.

[27] A.M. Pessi, J. Suonketo, M. Pentti, M. Kurkilahti, K. Peltola, A.R. Lehtimäki, Microbial Growth Inside Insulated External Walls as an Indoor Air Biocontamination Source, Appl. Environ. Microbiol. 68 (2) (2002) 963–967.
[28] A.A.H. Khan, S.M. Karuppayil, Fungal pollution of indoor environments and its management, Saudi J. Biol. Sci. 19 (2012) 405–426.
[29] K. Sterflinger, F. Pinzari, The revenge of time: fungal deterioration of cultural heritage with particular reference to books, paper and parchment, Environ. Microbiol. 14 (3) (2012) 559–566.
[30] R. Cataldo, A. De Donno, G. De Nunzio, G. Leucci, L. Nuzzo, S. Siviero, Integrated methods for analysis of deterioration of cultural heritage. The Crypt of "Cattedrale di Otranto", J. Cult. Herit. 6 (2005) 29–38.
[31] C. Balocco, G. Petrone, O. Maggi, C. Pasquarella, A CFD-based method for Biodeterioration Process Prediction in Historical Libraries and Archives, Int. J. Tech. Res. Appl. 3 (3) (2015) 307–319.
[32] C. Balocco, G. Pasquariello, O. Maggi, G. Crupi, S. Strippoli, P. Colaizzi, R. Albertini, C. Pasquarella, Microbial environmental monitoring in museums: preventive conservation of graphic collections, Conserv. Sci. Cult. Herit. Hist. Tech. J. 1 (2015) 275–289.
[33] S.P. Corgnati, M. Filippi, Assessment of thermo-hygrometric quality in museums: method and in-field application to the "Duccio di Buoninsegna" exhibition at Santa Maria della Scala (Siena-Italy), J. Cult. Herit. 11 (2010) 345–349.
[34] C. Pasquarella, C. Balocco, G. Pasquariello, G. Petrone, E. Saccani, P. Manotti, M. Ugolotti, F. Palla, O. Maggi, R. Albertini, A multidisciplinary approach to the study of cultural heritage environments: experience at the Palatina library in Parma, Sci. Total Environ. 536 (2015) 557–567.
[35] B.E. Launder, D.B. Spalding, The Numerical Computation of Turbulent Flows, Comput. Methods Appl. Mech. Eng. 3 (1974) 269–289.
[36] P. Deuflhard, A modified Newton method for the solution of ill-conditioned systems of nonlinear equations with application to multiple shooting, Numerical Math. 22 (1974) 289–315.
[37] F.Y. Zhao, E. Rank, D. Liu, H.Q. Wang, Y.L. Ding, Dual steady transports of heat and moisture in a vent enclosure with all round states of ambient air, Int. J. Heat Mass Transfer 55 (2012) 6979–6993.
[38] ISO 15927-4, Hygrothermal performance of buildings – Calculation and presentation of climatic data – Part 4: Hourly data for assessing the annual energy use for heating and cooling, 2005.
[39] A.F. Mills, Basic Heat and Mass Transfer, Prentice Hall Ed, London, 1990.
[40] F. Kreith, R.M. Manglik, M.S. Bohn, Principles of Heat Transfer, Cengage Learning, 2011.
[41] P.W. O'Callaghan, S.D. Probert, Sol-air temperature – Technical note, Appl. Energy 3 (4) (1977) 307–311.
[42] H. Hindmarsh, A.C. Brown, P.N. Grant, K.E. Lee, S.L. Serban, R. Shumaker, D.E. Woodward, C.S. Woodward, SUNDIALS: Suite of Nonlinear and Differential/Algebraic Equation Solvers, ACM Trans. Math. Software 31 (2005) 363–396.
[43] Comsol, Multiphysics User's Guide″ v. 5.0, Comsol Inc, 2015, http://www.comsol.com/.
[44] T.P. Labuza, C.R. Hyman, Moisture migration and control in multi-domain foods, Trends Food Sci. Technol. 9 (1998) 47–55.
[45] C. Hunter, C. Sanders, Mould, IEA Annex XIV, Condensation and Energy, Vol. 1, in: Chapter 2, 1991.
[46] IEA Annex 41 – MoistEng. Subtask 4 – 2007 Moisture-Engineering Application. Report of Energy Conservation in Buildings & Community, Systems Programme (ECBCS).
[47] D.M. Burch, W.C. Thomas, A.H. Fanney, Water vapor permeability measurements of common building materials, ASHRAE Trans. 98 (2) (1992) 9–16.
[48] R. Plagge, G. Scheffler, J. Grunewald, M. Funk, On the hysteresis in moisture storage and conductivity measured by the instantaneous profile method, J. Build. Phys. 2 (3) (2006) 247–259.
[49] A. Holm, H. Kunzel, K. Seldbauer, The hygrothermal behaviour of rooms: combining thermal building simulation and hygrothermal envelope calculation, in: VIII International IBPSA Conference, Eindhoven, The Netherlands, August 11–14, 2003, pp. 499–505.
[50] K. Sedlbauer, M. Krus, A new Model for Mould Prediction and its Application in Practice, Fraunhofer-Institute for Building Physics, Internal Report, Holzkirchen, Bavaria, Germany, 2001.
[51] K. Sedlbauer, M. Krus, K. Breuer, Mould Growth Prediction with a new Biohygrothermal Method and its application in practice. Fraunhofer-Institute for Building Physics, Internal Report, Holzkirchen, Bavaria, Germany, 2001.
[52] E. Vereecken, S. Roels, Review of mould prediction models and their influence on mould risk evaluation, Build. Environ. 51 (2012) 296–310.
[53] P.W. Mohr, S. Krawiec, Temperature Characteristics and Arrhenius Plots for Nominal Psychrophiles, Mesophiles and Thermophiles, J. Gen. Microbiol. 121 (1980) 311–317.
[54] W. Reichardt, R.Y. Morita, Temperature Characteristics of Psychrotrophic and Psychrophilic Bacteria, J. Gen. Microbiol. 128 (1982) 565–568.
[55] D.A. Ratkowsky, O. June, T.A. McMeekin, A. Ball, Relationship Between Temperature and Growth Rate of Bacterial, Cult. J. Bacteriol. 149 (1) (1982) 1–5.
[56] ANSI ASHRAE Standard-55, Thermal Environmental Conditions for Human Occupancy, ASHRAE Standards, USA, 2013.
[57] Z. Lin, Effective draft temperature for evaluating the performance of stratum ventilation, Build. Environ. 46 (2011) 1843–1850.
[58] C. Balocco, G. Petrone, G. Cammarata, Numerical multi-physical approach for the assessment of coupled heat and moisture transfer combined with people movements in historical buildings, Int. J. Build. Simulation 8 (2013) 2–9.